Available online at www.sciencedirect.com
ScienceDirect
Nuclear Instruments and Methods in Physics Research A 569 (2006) 175–179
NUCLEAR INSTRUMENTS & METHODS IN PHYSICS RESEARCH Section A
www.elsevier.com/locate/nima

Optimisation of scatter correction based on the use of partially transparent beam stoppers in PET

Keh-Shih Chuang[a,*], Hsing-Hon Lin[a], Jay Wu[b], Meei-Ling Jan[c]

[a]Department of Nuclear Science, National Tsing-Hua University, Taiwan, ROC
[b]Department of Radiological Technology, Central Taiwan University of Science and Technology, Taiwan, ROC
[c]Institute of Nuclear Science, Atomic Energy Council, Taiwan, ROC

Available online 22 September 2006

Abstract

To improve the counting efficiency, modern positron emission tomography scanners generally perform 3D data acquisition with the septa retracted. As a consequence, the scatter fraction can surge to as high as 40%. Our previous method proposed the use of a beam stoppers (BS) device to directly measure the scatter and to remove it from the sinogram. The BS partially attenuate the primary radiation of certain lines of response (LOR) without affecting the scattering events. To measure the scatter, dual scans are performed with and without the device in place. This study proposes an improved method. The dual scans are performed with the device placed at two different locations. The proposed method reduces the effective sampling distance without the need to actually increase the stopper's number. The scatter component at the LOR blocked by each stopper can be estimated. Assuming that the scattered radiation has a spatially slow-varying distribution, the whole scattered sinogram can be recovered using interpolation from these local measurements. Once the scatter component is estimated, the sinogram of the primary radiation can be obtained by subtracting the scatter component from the original data. The scatter free image is then reconstructed from the primary sinogram. This method was applied to scanned data of two digital phantoms using the Simulation System for Emission Tomography simulation package to demonstrate its effectiveness. Preliminary results showed that this method has slightly better performance than the previous BS method and the conventional single scatter simulation technique with smaller mean squared error and less noise in the corrected image.

PACS: 87.58.Fg

Keywords: PET; Scatter correction; Beam stopper; Sinogram; Partially transparent

1. Introduction

To improve the counting efficiency, modern positron emission tomography (PET) scanners generally perform 3D data acquisition with the septa retracted [1]. Scatter events are increased dramatically and scatter fraction is estimated to increase from 14% to 36% following septa retraction [2,3]. Rejection of scattered photons based on energy discrimination has limited success due to the poor energy resolution of PET camera detectors. Research and development efforts have largely focused on the scatter compensation required for quantitative 3D PET [1,4,5]. The most used correction is the simulation-based algorithm [6–8] called single scatter simulation (SSS) that estimate the scatter component via simulation. To achieve the desired accuracy, a prior knowledge of the activity distribution (both inside and outside the FOV) and of the density of the attenuation object is required. Furthermore, these approaches require considerable computational power and processing time because of the repetitive looping of numerous parameters.

In our previous study [9,10], we proposed the use of beam stoppers (BS) for PET scatter correction. Dual scans, with and without the stopper device, were used to obtain the scatter component. In this study, we propose an improved version to compensate the effect of increasing the number of BS. Instead of scanning with the removal of the

*Corresponding author. Tel.: +886 3 574 2681; fax: +886 3 571 8649.
E-mail address: kschuang@mx.nthu.edu.tw (K.-S. Chuang).

0168-9002/$ - see front matter © 2006 Elsevier B.V. All rights reserved.
doi:10.1016/j.nima.2006.08.105

stopper device, we perform the scan by placing the stopper device at different position. By doing so, we effectively reduce the sampling distance of the scatter spectrum without increasing the number of stoppers.

2. Materials and methods

In the following, we illustrate the proposed method using a 2D geometric setup, but this method could easily be extended to 3D cases.

2.1. Beam stopper

As seen in Fig. 1, several BS made of high Z material are placed between the detectors and the object. The stoppers partially block the recording of the true (primary) events without affecting the scatter radiation. The transmission fraction T can be obtained using air scans with the BS placed at two positions. Let the two device positions be denoted as L and R and let C_{L0} and C_{R0} be the counts of the air scans at these two positions. Then

$$T_R(t,\theta) = C_{R0}(t,\theta)/C_{L0}(t,\theta) \quad (1)$$

for those lines of responses (LOR) intersecting with the BS at projection angle θ and distance t equal to

$$t_{Ri}(\theta) = x_{Ri}\cos\theta + y_{Ri}\sin\theta \quad (2)$$

where (x_{Ri}, y_{Ri}) is the coordinate of the ith BS at the R-set position, and $T_R(t,\theta) = 1$ for those LORs that do not intersect with the BS. Similarly, we have

$$T_L(t,\theta) = C_{L0}(t,\theta)/C_{R0}(t,\theta). \quad (3)$$

Let S and P represent the scattered and primary components of the original signal, and C_L and C_R represent the counts in the sinogram at two scanning positions. Then

$$C_L(t,\theta) = T_L(t,\theta)\times P(t,\theta) + S(t,\theta) \quad (4)$$

$$C_R(t,\theta) = T_R(t,\theta)\times P(t,\theta) + S(t,\theta). \quad (5)$$

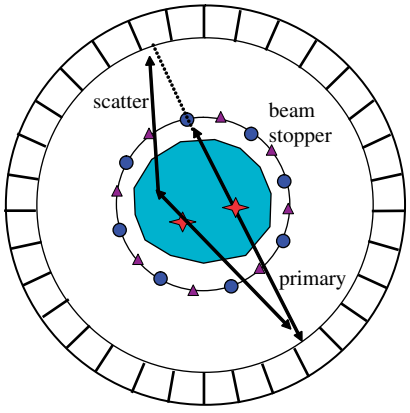

Fig. 1. Geometry of the system with the beam stoppers device. The stoppers partially block the primary radiations without affecting the scattered radiations. ○ and Δ mark the positions of stopper device at two different scans.

The scattered component for the LOR at (t,θ) can be obtained by

$$S(t_{Ri},\theta) = \frac{T_R(t_{Ri},\theta)\times C_L(t_{Ri},\theta) - T_L(t_{Ri},\theta)\times C_R(t_{Ri},\theta)}{T_R(t_{Ri},\theta) - T_L(t_{Ri},\theta)}. \quad (6)$$

Note that $T_R(t_{Ri},\theta) < 1$ and $T_L(t_{Ri},\theta) = 1$. Similarly

$$S(t_{Li},\theta) = \frac{T_L(t_{Li},\theta)\times C_R(t_{Li},\theta) - T_R(t_{Li},\theta)\times C_L(t_{Li},\theta)}{T_L(t_{Li},\theta) - T_R(t_{Li},\theta)}. \quad (7)$$

The entire distribution of scattered radiation, $S(t,\theta)$, can be recovered through cubic spline interpolation from $S(t_{Ri},\theta)$ and $S(t_{Li},\theta)$ for $i = 1, n$, where n is the total number of stoppers. The scattered event calculated is then smoothed using a 7×7 Gaussian filter. Two primary sinograms can be obtained by subtracting the scattered event from their original sinograms, i.e.

$$P_R(t,\theta) = [C_R(t,\theta) - S(t,\theta)]/T_R(t,\theta) \quad (8)$$

and

$$P_L(t,\theta) = [C_L(t,\theta) - S(t,\theta)]/T_L(t,\theta). \quad (9)$$

These two primary sinograms are then summed together and reconstructed to yield the scatter free image.

2.2. Digital phantom

Two digital phantoms are used for this study: a Utah multi-compartment cylindrical (radius = 17 cm) phantom (Fig. 2) and an anthropomorphic Zubal phantom (Fig. 3). In the Utah phantom, four compartments (A, B, C, and D)

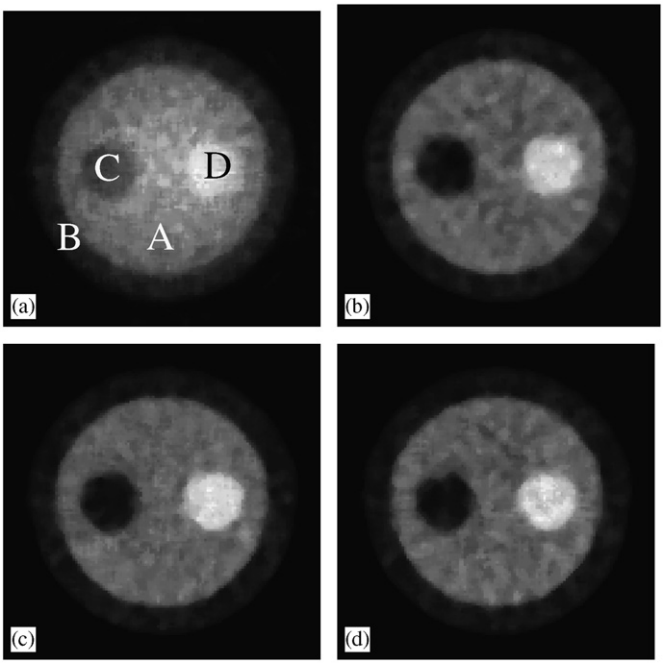

Fig. 2. Utah phantom: the uncorrected image (a) and images corrected by SSS method (b), BS method with $n = 4$ (c), and BSR method with $n = 4$ (d).

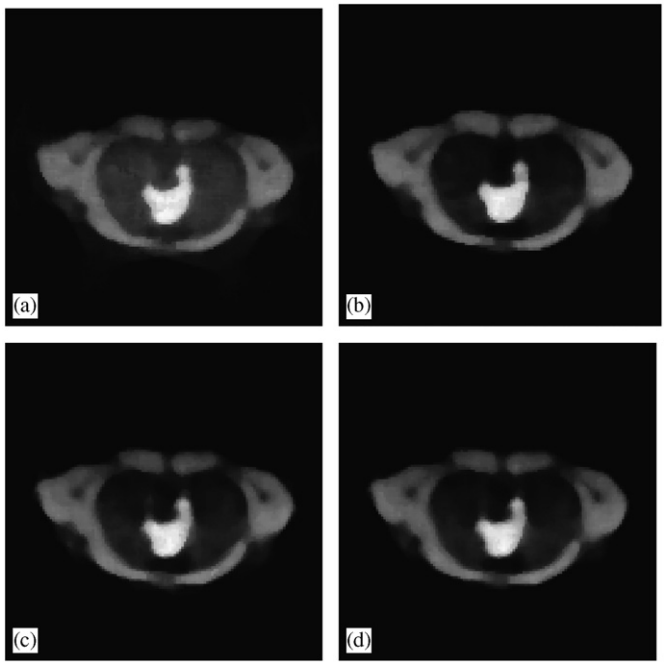

Fig. 3. Zubal phantom: the uncorrected image (a) and images corrected by SSS method (b), BS method with $n = 8$ (c), and BSR method with $n = 8$ (d).

each with a height of 20 cm were water-filled with individual relative activities of 5:1:1:10 per unit volume. In the Zubal phantom, three types of tissues including lung, blood pool, and soft tissue were filled with activity concentrations of 0.37, 3.7, and 1.85 MBq/cc, respectively. The size of the phantom is 32 and 18 cm in long and short axes.

The simulation is performed using the Simulation System for Emission Tomography (SIMSET) code from the University of Washington [11].

The BS device is a birdcage comprising of a various number of cylindrical leads arranged uniformly on a cylindrical surface. The stopper with radius equal to 0.3 cm is used during this study as our previous results [9] indicate that it yields the best results. The radius of the birdcage cylinder is 18.44 cm to cover the phantoms under study. Two simulations are performed with the BS device rotated to an angle such that the two stoppers are interleaved with each other (Fig. 1).

The total number of photons emitted are 2.0×10^{10} and 1.0×10^{9} for the air and object scans, respectively. The total photons emitted in the simulation with and without the BS are equal to one half of that used for the regular scans.

2.3. Image quality assessment

The reconstructed image is normalized such that the total pixel value is equal to the total photons emitted from the phantom. The mean squared error (MSE) and normalized standard deviation (NSD) are calculated for the reconstructed images to assess the performance of the scatter correction method. The MSE is defined as the mean of the squared activity differences between the reconstructed image and the digital phantom. It measures the accuracy of the scatter correction method. Moreover, the NSD is the ratio between the standard deviation and average activity measured in the background regions of the reconstructed image. It represents the noise in the resultant image.

3. Results

The resultant image corrected by the previous beam stopper method (denoted as BS), rotated beam stopper technique (BSR), and SSS [8] are compared. For each case, six studies are performed. Fig. 2 shows the results of the Utah phantom study. Clearly, the images corrected by all three techniques exhibit a more uniform background and better contrast. Fig. 4 illustrates the horizontal profiles across the center of the images ($y = 64$) in Fig. 2. Clearly, all correction techniques approximate the simulated values closely to the phantom.

Fig. 3 displays the results of the scatter correction for the Zubal phantom and Fig. 5 plots their horizontal profiles across the central bodies. It can be seen that both BS and SSS methods fully restore the tissue activity values.

Various numbers ($n = 4$, 8, 12) of stoppers were used in the simulation on the same phantom to determine a reasonable number for the stoppers. Table 1 compares the measurements of the MSE for the Utah phantom and Zubal phantom, using various scatter correction methods. All methods display significant improvements in the MSE of the reconstructed images compared to the original. The BSR method shows the lowest MSE among the three while the BS method performs better than SSS algorithm when suitable number of stoppers is used. When the stoppers number is too small, the MSE of the BS corrected image is larger than SSS algorithm. This is due to fact that the

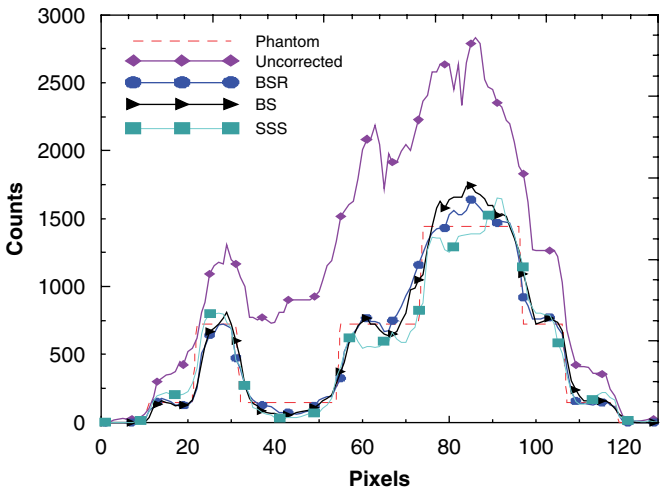

Fig. 4. Profiles drawn (at $y = 64$) across the Utah phantom, the image of the original (uncorrected), and scatter corrected images by SSS, BS, and BSR.

larger distance in scatter distribution interpolation causes larger error. Due to the fact that the structure of the Zubal phantom is much complex than the Utah phantom, the assumption of linear relation of scattering between sampling points is no longer true and the performances of both BS methods are degraded for the Zubal phantom. Based on the same reasoning, the Zubal phantom requires more stoppers than the Utah phantom for optimal performance.

Table 2 lists measurements of the NSD for the two phantoms using various scatter correction methods. For both BS and BSR method, the photons absorption by the stoppers causes the noise to be increased with the stopper number. Also note that the noise in the SSS corrected image is higher than images generated by both BS methods. This is probably due to the fact that SSS require the calculation of scaling factor from outside the body, which is noise. The BS methods require two scans each with half of the scan time. The Poisson noise will be greater for each scan compared to the original data. However, since these two data sets are summed together to generate the primary sinogram, the statistical noise in the projection data is basically the same as in the original data.

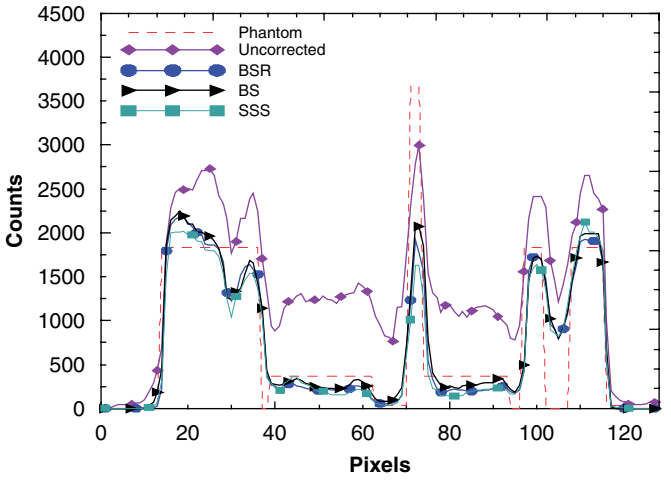

Fig. 5. Profiles drawn (at $y = 64$) across the Zubal phantom, the image of the original (uncorrected), and scatter corrected images by SSS, BS, and BSR.

4. Discussion

For a simple object, the scattered distribution function between the two locations of stoppers can be estimated by a low order function. However, as the object becomes more complex, the linear distribution of the scatter radiation no longer holds. To compensate for this effect, the number of stoppers around the subject needs to be increased to reduce the separations between stoppers. However, the scatter induced in the stoppers and the scatter absorbed by the stoppers also increases with the number of stoppers. This will increase errors in the scatter correction method. As a result, there exist a reasonable number of stoppers for optimal results, depending on the size and homogeneity of the subject under study. The proposed method effectively decreases the distance between sampling points without increasing the number of stoppers. As expected, the results show that both BS methods yield the same MSE when the stopper number of BSR is only half of that as with BS. Furthermore, it is noticed from the experiments that for equal MSE, the BSR generates images with smaller noise (NSD) than the BS method. The noise is more significant when more stoppers are used which absorbs more photons and causes the increase in the quantum noise.

Note that in this study, the axial extents of both phantoms are set to be equal to the axial FOV, i.e., no scatters are originated from OFOV. Otherwise, the result of SSS will be worsened as the technique does not compensate for OFOV scatter.

5. Conclusions

This study proposes an improved scatter correction method for the PET system using partially transparent BS. The proposed method possesses the same properties (i.e., direct, fast, and simple) in scatter correction as the

Table 1
The average mean squared error (MSE $\times 10^4$) of six studies with various scatter correction techniques for the Utah phantom and Zubal phantom

	Uncorrected	SSS	BSR ($n = 4$)	BSR ($n = 8$)	BSR ($n = 12$)	BS ($n = 4$)	BS ($n = 8$)	BS ($n = 12$)
Utah	22.927±0.336	0.764±0.029	0.691±0.028	0.720±0.020	0.813±0.020	0.788±0.048	0.692±0.014	0.718±0.030
Zubal	21.376±0.153	9.104±0.103	9.076±0.079	8.977±0.116	8.950±0.098	9.437±0.127	9.123±0.095	9.060±0.109

Table 2
The average normalized standard deviation (NSD) of six studies using scatter correction with various scatter correction techniques for the Utah phantom and Zubal phantom (measured at the lower right lung region)

	Uncorrected	SSS	BSR ($n = 4$)	BSR ($n = 8$)	BSR ($n = 12$)	BS ($n = 4$)	BS ($n = 8$)	BS ($n = 12$)
Utah	0.123±0.007	0.114±0.009	0.088±0.003	0.098±0.017	0.111±0.016	0.086±0.008	0.107±0.008	0.098±0.004
Zubal	0.280±0.019	0.369±0.033	0.274±0.016	0.336±0.029	0.382±0.047	0.273±0.011	0.313±0.026	0.316±0.044

previous version [9]. The new method reduces the effective sampling distance without increasing the number of stoppers. The results indicate that this method outperforms the SSS with lower noise and MSE in the corrected image. Furthermore, the new method makes it easier to switch stopper position during the scan in practical implementation.

References

[1] D.W. Townsend, A. Geissbuhler, M. Defrise, E.J. Hoffman, T.J. Spinks, D.L. Bailey, M.C. Gilardi, IEEE Trans. Med. Img. 10 (1991) 505.
[2] T.J. Spinks, T. Jones, D.L. Bailey, D.W. Townsend, S. Grootoonk, P.M. Bloomfield, M.C. Gilardi, M.E. Casey, B. Sipe, J. Reed, Phys. Med. Biol. 37 (1992) 1637.
[3] C.C. Watson, D. Newport, M.E. Casey, R.A. deKemp, R.S. Beanlands, M. Schmand, IEEE Trans. Nucl. Sci. NS-44 (1997) 90.
[4] S. Grootoonk, T.J. Spinks, D. Sashin, N.M. Spryou, T. Jones, Phys. Med. Biol. 41 (1996) 2757.
[5] R.J. Jaszczak, K.L. Greer, C.E. Floyd, C.C. Harris, R.E. Coleman, J. Nucl. Med. 25 (1984) 893.
[6] C.C. Watson, IEEE Trans. Nucl. Sci. NS-47 (2000) 1587.
[7] C.S. Levin, M. Dahlbom, E.J. Hoffman, IEEE Trans. Nucl. Sci. NS-42 (1995) 1181.
[8] J.M. Ollinger, Phys. Med. Biol. 41 (1996) 153.
[9] K.S. Chuang, J. Wu, M.L. Jan, S. Chen, C.H. Hsu, Nucl. Instr. Meth. A 551 (2005) 540.
[10] J. Wu, K.S. Chuang, C.H. Hsu, M.L. Jan, I.M. Hwang, T.J. Chen, Phys. Med. Biol. 50 (2005) 4593.
[11] R.L. Harrison, S.D. Vannoy, D.R. Haynor, S.B. Gillispie, M.S. Kaplan, T.K. Lewellen, in: Conference Record, 1993 IEEE Nuclear Science Symposium.